

Searching for Inflationary B-modes: Can dust emission properties be extrapolated from 350 GHz to 150 GHz?

Konstantinos Tassis^{1,2} * and Vasiliki Pavlidou^{1,2}

¹*Department of Physics and ITCP, University of Crete, 71003 Heraklion, Greece*

²*Foundation for Research and Technology - Hellas, IESL, Voutes, 7110 Heraklion, Greece*

2 July 2018

ABSTRACT

Recent *Planck* results have shown that radiation from the cosmic microwave background passes through foregrounds in which aligned dust grains produce polarized dust emission, even in regions of the sky with the lowest level of dust emission. One of the most commonly used ways to remove the dust foreground is to extrapolate the polarized dust emission signal from frequencies where it dominates (e.g., ~ 350 GHz) to frequencies commonly targeted by cosmic microwave background experiments (e.g., ~ 150 GHz). In this paper, we describe an interstellar medium effect that can lead to decorrelation of the dust emission polarization pattern between different frequencies due to multiple contributions along the line of sight. Using a simple 2-cloud model we show that there are two conditions under which this decorrelation can be large: (a) the ratio of polarized intensities between the two clouds changes between the two frequencies; (b) the magnetic fields between the two clouds contributing along a line of sight are significantly misaligned. In such cases, *the 350 GHz polarized sky map is not predictive of that at 150 GHz*. We propose a possible correction for this effect, using information from optopolarimetric surveys of dichroically absorbed starlight.

Key words: cosmology: inflation – polarization – ISM: magnetic fields – ISM: dust – cosmic background radiation – cosmology: observations

1 INTRODUCTION

The recently claimed detection, at high confidence, of B-modes in cosmic microwave background (CMB) polarization that cannot be attributed to lensed E-modes by the BICEP2 experiment (Bicep2 Collaboration 2014) was greeted with both enthusiasm and caution. If all or part of this B-mode signal were confirmed to be primordial, it would constitute the first detection of a smoking-gun for inflation, a direct probe of yet-unknown physics such as quantum gravity, and thus one of the most important discoveries in astrophysics, cosmology, and high-energy physics in the past several decades. However, a joint analysis of BICEP2 and *Planck* data (BICEP2/Keck et al. 2015) showed that most, if not all, of the BICEP2 signal was the result of the most severe, ever-present contaminant in the studies of CMB polarization: polarized emission from interstellar dust. This development does not slow down the search for primordial B-modes; but it does highlight the need for a much-enhanced ability to understand and subtract foregrounds.

Planck has now established that even in sky regions away from the Galactic plane, where the dust emission is

minimum, the primordial B-mode signal is below that of dust (Planck Collaboration 2014d). In order for a future B-mode experiment to detect a primordial signal, the polarized emission from interstellar dust and its polarization pattern will have to be subtracted from the CMB sky at high accuracy. Any systematic errors entering this correction will need to be carefully considered: even if they are small compared to the level of the dust signal, they may be important compared to the (currently unknown) level of the primordial signal. It is such a systematic effect that we describe here.

Currently the subtraction of the dust signal is based on measuring polarized emission from dust at frequencies where it is dominant (e.g., ~ 350 GHz) and extrapolating the dust polarization pattern to frequencies dominated by the CMB and targeted by CMB experiments (60 - 150 GHz). The basis of this approach is that the dust emission spectrum is reasonably well-understood (typically represented by a modified blackbody spectrum); and thus the dust polarization pattern measured at 350 GHz can be extrapolated to lower frequencies (Planck Collaboration 2014d). The polarization direction at 350 GHz is dictated by the magnetic field threading the interstellar clouds where the dust resides. If for example all emission originates from a single cloud, then the emission will be partially polarized in a direction per-

* tass@physics.uoc.gr

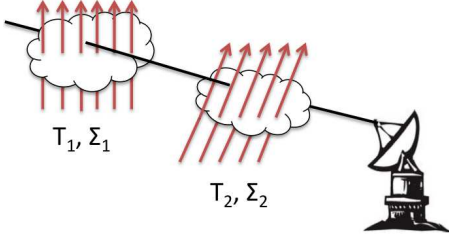


Figure 1. Two clouds with temperatures T_1 and T_2 , dust column densities Σ_1 and Σ_2 , and magnetic fields oriented at different directions contribute to the total dust-emission intensity along a line of sight.

pendicular to the plane-of-the-sky (POS) projection of the magnetic field. The dust emission at 150 GHz should then be polarized in the same direction - since the polarization is generated by that same magnetic field.

The validity of such an extrapolation breaks down whenever more than one “cloud” (more than one dusty region with different temperatures and magnetic fields) is contributing to the integrated signal along the line of sight. The reason is that the total linearly polarized intensity fraction and polarization direction is obtained by algebraic addition of each of the Stokes linear polarization parameters Q , U , and I along the line of sight. If the relative contribution from two regions with different polarization directions (effectively different magnetic field directions) changes between frequencies, so will the resulting polarization fraction and polarization direction. Indeed, the relative contribution *will* change between frequencies if the two regions have different temperatures, due to the temperature-dependent black-body part of the dust emission spectrum.

In this paper we use a simple two-cloud model to demonstrate that this effect could cause decorrelation of the polarization pattern between 350GHz and 150GHz maps. We calculate conditions under which the effect would be large in configuration (rather than in Fourier) space. And we propose ways to correct for this systematic effect.

2 TWO-CLOUD MODEL

We consider a simple case in which only two “clouds” of temperatures T_1 and T_2 and dust column densities Σ_1 and Σ_2 contribute to the total dust emission along a line of sight (see Fig. 1). The total intensity emitted by each cloud can be generally well described by a modified black-body spectrum (Hildebrand 1983; Planck Collaboration et al. 2014; Planck Collaboration 2014c),

$$I_\nu = B_\nu(T) [1 - \exp(-\kappa\Sigma)], \quad (1)$$

where $B_\nu(T)$ is the blackbody spectral radiance and κ is the opacity.

If the degree of polarization in a cloud is p , then the polarized intensity will be pI . In this paper we assume that p is independent of frequency, although in the general case this is not so (Serkowski et al. 1975). In the case of low optical depth $\kappa\Sigma$ (appropriate for regions of low dust emission, such as the low-dust-emission regions typically targeted by CMB

experiments), the ratio of polarized intensities contributed by each cloud can be written as

$$\rho_\nu = \frac{I_1 p_1}{I_2 p_2} = \frac{B_\nu(T_1) \Sigma_1 p_1}{B_\nu(T_2) \Sigma_2 p_2}. \quad (2)$$

This will be a function of frequency because of the blackbody part of the emission spectrum.

The polarization state of the dust emission from each cloud can be completely described by the Stokes parameters Q , U , and I (where I is the total intensity). The polarization degree p and polarization angle χ of the emission from a single cloud are related to the Stokes parameters through

$$p = \frac{\sqrt{Q^2 + U^2}}{I}, \quad \tan 2\chi = \frac{U}{Q}. \quad (3)$$

When both clouds contribute to the emission along a given line of sight, the corresponding Stokes parameters add:

$$Q_{\text{tot}} = Q_1 + Q_2, \quad U_{\text{tot}} = U_1 + U_2, \quad I_{\text{tot}} = I_1 + I_2. \quad (4)$$

The polarization degree p_{tot} and electric vector position angle χ_{tot} of the total emission then are obtained by inserting Q_{tot} , U_{tot} , and I_{tot} into Eq. (3).

If the POS-projection of the magnetic field in cloud 1 lies in a direction forming an angle α with that of cloud 2, the polarization directions of each cloud’s emitted radiation will similarly form an angle α . Without loss of generality, we can take the magnetic field of cloud 1 to be at an angle $\chi_1 = \alpha/2$ from the reference direction, and that of cloud 2 to be at an angle $\chi_2 = -\alpha/2$. Then $\tan 2\chi_1 = \tan \alpha$, $\tan 2\chi_2 = -\tan \alpha$, and $p_i = |Q_i| \sqrt{1 + \tan^2 \alpha} / I_i$ in both cases ($i = 1, 2$). We can represent this configuration with Stokes parameters

$$I_1 = I_2 \rho_\nu (p_2/p_1), \quad Q_1 = \frac{\rho_\nu p_2 I_2}{\sqrt{1 + \tan^2 \alpha}}, \quad U_1 = \frac{\rho_\nu p_2 I_2 \tan \alpha}{\sqrt{1 + \tan^2 \alpha}} \quad (5)$$

and

$$I_2, Q_2 = \frac{p_2 I_2}{\sqrt{1 + \tan^2 \alpha}}, \quad U_2 = -\frac{p_2 I_2 \tan \alpha}{\sqrt{1 + \tan^2 \alpha}}, \quad (6)$$

where we have taken $Q_1, Q_2 > 0$, and U_1, U_2 carry the signs. The Stokes parameters of the total signal will then be

$$Q_{\text{tot}} = \frac{p_2 I_2 (\rho_\nu + 1)}{\sqrt{1 + \tan^2 \alpha}}, \quad U_{\text{tot}} = \frac{p_2 I_2 (\rho_\nu - 1) \tan \alpha}{\sqrt{1 + \tan^2 \alpha}}, \quad (7)$$

$$I_{\text{tot}} = I_2 (1 + \rho_\nu p_2/p_1).$$

The resulting polarization parameters will thus be

$$\tan 2\chi_{\text{tot}} = \tan \alpha \frac{(\rho_\nu - 1)}{(\rho_\nu + 1)}$$

$$p_{\text{tot}} = \frac{p_2}{1 + \rho_\nu p_2/p_1} \sqrt{\frac{(\rho_\nu + 1)^2 + \tan^2 \alpha (\rho_\nu - 1)^2}{1 + \tan^2 \alpha}}. \quad (8)$$

We next consider the two extreme cases of relative magnetic field directions: parallel and perpendicular.

2.1 Magnetic fields parallel

The simplest and least problematic case is the one where the directions of the POS magnetic field, and thus the polarization directions, are parallel in the two clouds (i.e. $\alpha = 0$). In this case, Eqs. (8) reduce to

$$\tan 2\chi_{\text{tot}} = 0, \quad p_{\text{tot}} = \frac{p_1 p_2 (\rho_\nu + 1)}{p_1 + \rho_\nu p_2}, \quad (9)$$

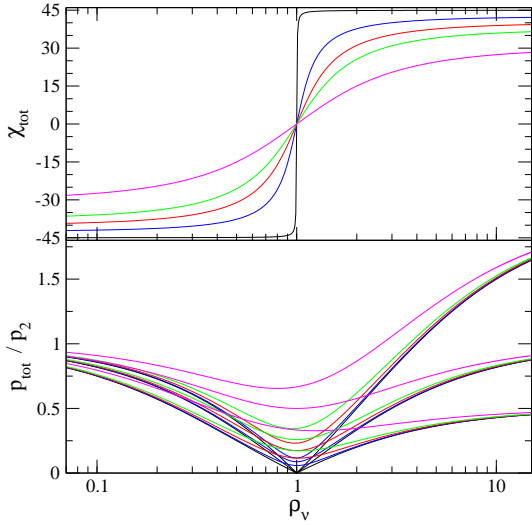


Figure 2. Upper panel: χ_{tot} as a function of ρ_ν for different values of angle α between the POS magnetic fields of the clouds: black: $\approx 90^\circ$; blue: 85° ; red: 80° ; green: 75° ; magenta: 60° . Lower panel: p_{tot}/p_2 as a function of ρ_ν . Colours as above. Three different cases are shown, with $p_2/p_1 = 0.5$, $p_2/p_1 = 1$, and $p_2/p_1 = 2$, distinguished by their different asymptotic behavior at high ρ_ν , when $p_{\text{tot}} \rightarrow p_1$.

which simplifies to $p_{\text{tot}} = p_0$ if $p_1 = p_2 = p_0$. If the polarization properties of both clouds are the same, the resulting combined emission will also share these properties.

2.2 Magnetic fields perpendicular

Conversely, the most worrisome case is the one where the POS-projection of the magnetic field in cloud 1 lies in a direction perpendicular to that in cloud 2. In this case, $\tan \alpha \rightarrow \infty$, so from Eqs. (8) we obtain

$$\chi_{\text{tot}} \approx 45^\circ \text{sgn}(\rho_\nu - 1), p_{\text{tot}} \approx \frac{p_1 p_2 |\rho_\nu - 1|}{p_1 + \rho_\nu p_2}. \quad (10)$$

The polarization angle $\tan 2\chi_{\text{tot}} \rightarrow \infty$ and $\chi \rightarrow 45^\circ$ if cloud 1 dominates in polarized emission; conversely, $\tan 2\chi_{\text{tot}} \rightarrow -\infty$ and $\chi \rightarrow -45^\circ$ if cloud 2 dominates in polarized emission. If $\rho_\nu - 1$ retains the same sign between two frequencies, the resulting polarization angles will be the same. If $\rho_\nu - 1$ changes sign, the resulting polarization angles *will abruptly rotate by 90° as one changes from one frequency to another.*

3 RESULTS

The behavior of χ_{tot} and p_{tot} as a function of the ratio of polarized intensities, ρ_ν , between the two clouds, is demonstrated in Fig. (2). When $\rho_\nu \ll 1$, cloud 2 dominates, and both χ_{tot} and p_{tot} tend to the corresponding cloud 2 values; conversely, when $\rho_\nu \gg 1$, cloud 1 dominates. As a result, the maximum change in χ_{tot} as ρ_ν changes is in all cases equal to α . This maximum change occurs when we transition from cloud 1 completely dominating the polarized emission to cloud 2 dominating. The larger the angle α , the more abrupt the transition between the two regimes, which occurs at $\rho_\nu = 1$. The resulting polarization fraction p_{tot} is plotted in units of p_2 , and for three values of p_1 : $p_1 = p_2/2$,

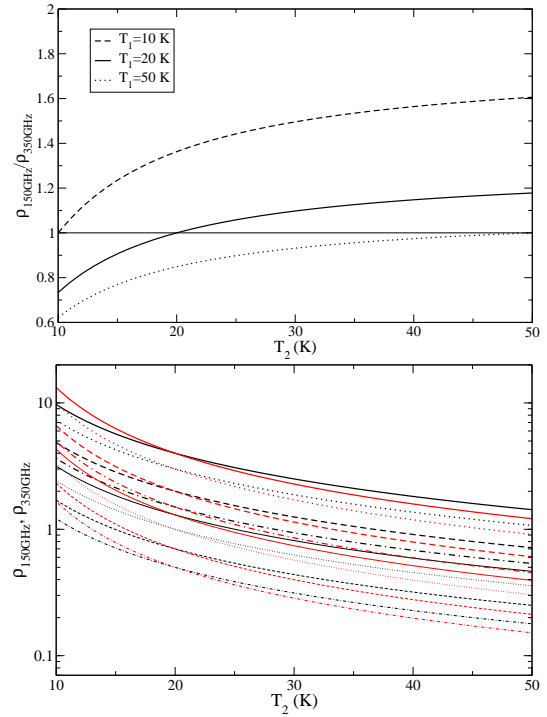


Figure 3. Upper panel: ratio of polarized intensities ρ at 350 GHz and 150 GHz as a function of cloud 2 temperature, for three different cloud 1 temperatures. Lower panel: Ratio ρ at 150 GHz (black) and 350 GHz (red), as a function of cloud 2 temperature. Cloud 1 temperature is fixed at 20 K. Line type corresponds to different values of the product $(\Sigma_1/\Sigma_2)(p_1/p_2)$: dot-dash: 0.5; dash: 0.7; dot: 1; solid: 1.3; thick dot-dash: 1.5; thick dashed: 2; thick dot: 3; thick solid: 4.

$p_1 = p_2$, and $p_1 = 2p_2$, distinguished in the plot by the different asymptotic behavior of the $p_{\text{tot}}(\rho_\nu)$ curves as cloud 1 dominates (for $\rho_\nu \gg 1$). The possible change in p_{tot} as ρ_ν changes is larger the larger the angle α and the larger the difference between p_1 and p_2 . As discussed in §2.2, for the extreme case $\alpha \rightarrow 90^\circ$, the resulting POS magnetic field has a step-function behavior between -45° for $\rho_\nu < 1$, and $+45^\circ$ for $\rho_\nu > 1$, while the resulting polarization fraction passes through zero at $\rho_\nu = 1$.

In conclusion, the potential change of the observed polarization properties of the combined emission from the two clouds, between 150 and 350 GHz, depends on the change in ρ_ν between the two frequencies. In turn, from Eq. (2), ρ_ν depends on the temperature of the two clouds, the ratio of their column densities, and the ratio of their polarization fractions. Note that ρ_ν *does not* depend on the ratio of temperatures T_1/T_2 , but has a more complicated dependence through the exponential part of the Planck law. In fact, when both clouds are hot enough to be in their Rayleigh-Jeans regime in the frequencies of interest, and the dependence of ρ_ν on the temperature is dominated by the T_1/T_2 ratio, the frequency dependence of ρ_ν cancels out, ρ_ν remains unchanged between 150 and 450 GHz, and the polarization properties of the resulting emission remain constant. However, dust in typical ISM temperatures (~ 20 K) is *not* in the Rayleigh-Jeans limit between 150 and 350 GHz. Possible values of ρ_ν for interstellar medium clouds, for different temperatures of the two clouds and different values of the

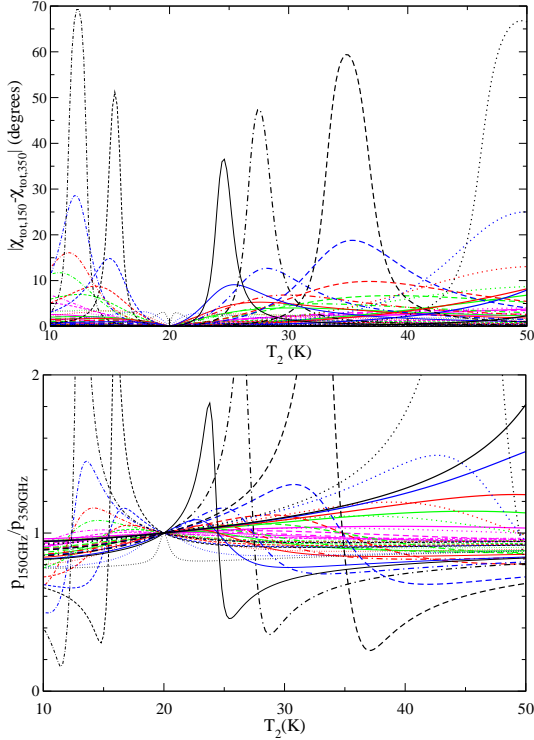


Figure 4. Upper panel: difference of polarization angles of combined signal as measured at 350 GHz and 150 GHz, as a function of cloud 2 temperature. Lower panel: ratio of polarization fractions of combined signal as measured at 350 GHz and 150 GHz as a function of cloud 2 temperature, assuming $p_1 = p_2$. Color corresponds to angle α between the POS magnetic fields of the clouds: black: $\approx 90^\circ$; blue: 85° ; red: 80° ; green: 75° ; magenta: 60° . Line types as in Fig. 3 (lower).

product $(\Sigma_1/\Sigma_2)(p_1/p_2)$, as well as likely changes of ρ_ν between 150 and 350 GHz are shown in Fig. 3.

The manner in which the polarization properties measured for the combined signal change between 350 GHz and 150 GHz is shown in Fig. 4. Different colours correspond to different angles α between the POS magnetic fields of the two clouds as in Fig. 2, and different line types to different values of the product $(\Sigma_1/\Sigma_2)(p_1/p_2)$, as in Fig. 3. The upper panel shows the difference of the polarization angle of the combined signal as measured between 150 GHz and 350 GHz, and the lower panel shows the ratio $p_{150\text{GHz}}/p_{350\text{GHz}}$, plotted in both cases against the temperature of cloud 2. The temperature of cloud 1 is fixed at the average interstellar dust value of 20 K (Planck Collaboration 2014b). In the case of the degree of polarization, we have taken $p_1 = p_2$, and the true effect may thus be even greater (see Fig. 2, lower panel).

The first point to note is that once we consider the possible polarization pattern decorrelation as a function of all parameters entering the problem, a large range of outcomes is possible. The physically transparent picture depicted in Fig. (2) becomes much more complicated. However, there are still generally informative trends.

When the temperatures of the two clouds are different, severely misaligned cloud magnetic fields will result in significant differences in polarization degree and polarization angle between 150 GHz and 350 GHz for a range of possible

parameters of our model. Caution is then warranted when using 350 GHz data to extrapolate dust properties to 150 GHz, as the 150 GHz polarized emission map might look very different from the 350 GHz map. The polarization degree might differ by large factors (more than a factor of 2 for the most misaligned magnetic fields, more than 20% if the POS magnetic field of the two clouds forms an angle higher than 75°). Similarly, the polarization angle can be up to 90° different if the clouds are perfectly misaligned, and certainly higher than 20° for clouds with severely but not perfectly misaligned POS magnetic fields ($\sim 85^\circ$).

On the other hand, there are large parts of the parameter space where the polarization properties of the combined emission would look very similar at the two frequencies: if the POS magnetic fields of the two clouds form an angle of less than 60° , then the difference in polarization fraction is less than 10% and the difference in polarization angle less than 5° , independently of the other parameters of our model. This behavior, as discussed in the next section, offers a straightforward way to correct for this systematic effect, by masking problematic regions with severe magnetic field misalignments along the line of sight.

4 DISCUSSION

The effect we have discussed here is intrinsic to all microwave experiments and is due to information loss due to line-of-sight integration. Future experiments with greater sensitivity/angular resolution will not avoid this systematic uncertainty. However, if the magnetic fields of the contributing clouds form an angle smaller than 60° , then the resulting change in the polarization properties maps from 350 GHz to 150 GHz is minimal (at least under the assumptions of the simple model considered here).

Our model can be improved in a variety of ways: e.g., more than two contributing clouds along the line of sight, a physical model of dust properties and emission, and constraining the observed combined emission spectrum along a line of sight to agree within uncertainties with the observed one. Additionally, in our model we assumed the degree of polarization to be constant across frequencies, and the frequency dependence of the dust opacity to be identical in the two clouds. Any deviation from these assumptions will cause further change between frequencies in the ratio ρ_ν of polarized emission between the two clouds. Further change in ρ_ν will cause further discrepancies between the maps in the two frequencies, up to the maximum difference, which is the difference between a state where cloud 1 completely dominates the polarized emission, and a state where cloud 2 completely dominates.

There are two ways for future experiments to deal with the systematic effect we have identified here. The first is to calculate, for the specifications for each experiment, the magnitude of the error introduced by this effect in Fourier space, and determine whether it is comparable to the level of the primordial signal they might claim. This would involve simulating the effect using a detailed dust emission model, a simulated 3-dimensional map of high-Galactic-latitude interstellar clouds and their magnetic fields, and the specific instrument response functions, mapping frequencies, and analysis techniques. The second is to correct for the effect.

Although a detailed analysis in Fourier space is beyond the scope of this letter, some empirical data do exist addressing polarization pattern decorrelation of the dust signal between different frequencies in Fourier space. Cross-correlation studies of the polarized microwave sky between frequencies performed by Planck Collaboration (2014b) are limited to mid Galactic latitudes (lower than those targeted by CMB B-mode experiments) and average on larger (10°) scales than those relevant for primordial B-modes. Mid latitudes are likely to be less decorrelated, because a larger number of clouds is likely to be present along each line of sight, which more frequently than not will average out the strong variations that are possible in the case of only two clouds. Similar studies in Planck Collaboration (2014d) at higher latitudes are limited to a smaller frequency difference (between 353 and 217 GHz instead of 353 and 150). For larger frequency differences, the decorrelation will be larger, because the difference in polarized emission fraction from each cloud will be larger (see Fig. (2)). Even so, the 1σ pattern decorrelation ratio between 353 and 217 GHz is found to be at 3% (of the dominant dust signal); assuming that it would similarly be $\gtrsim 3\%$ at CMB B-mode mapping frequencies, if the primordial signal is at 30% of the dust, the systematic discussed here would be at 10% of the primordial signal, and if the primordial signal is at 3% of the dust, the systematic would be at the 100% level. Depending on the level of primordial signal, this effect could be of little concern, or very problematic.

In configuration space, data are similarly not very constraining. If we were to make the simplistic assumption that each line of sight in a CMB B-mode experiment experiences polarized dust emission from two clouds and the magnetic fields in these clouds are randomly (uniformly) distributed, then the probability of a large, problematic ($> 60^\circ$) misalignment of magnetic fields is 33%. The realistic scenario is much more complicated: the probability of severe misalignments depends on the number of clouds within the Galactic disk projected to high latitudes, the number of higher-distance high-velocity clouds that may also intervene along specific lines of sight, the size of each of these clouds, the correlation length of the magnetic field within a single cloud, and large-scale correlations of the magnetic field within the Galactic disk. Certainly the sky at high latitudes appears “patchy” on the plane of the sky (Planck Collaboration 2014a). By Copernican arguments (see also Planck Collaboration 2014b; Planck Collaboration et al. 2014), it will also be patchy along the line of sight, with several distinct clouds, each with its own, potentially different, magnetic field. Additionally, at high latitudes, interstellar clouds are most likely to be located nearby, from a few tens of parsecs to one Galaxy scale height (few hundred parsecs), and thus span large angular scales. (e.g., the Polaris flare cloud, André et al. 2010, over 10° across, Galactic latitude b up to 30° , and the Leo cloud, Peek et al. 2011, $\sim 10^\circ$ across, b up to 50°). Halo objects can also emit in microwave frequencies (e.g. high velocity clouds, such as IVC 135+53, Lenz et al. 2015 with b up to 60° , 8° across). Only a few severe misalignments between such large (in angular scale) clouds may end up affecting a large fraction of the CMB sky.

This systematic effect could, however, be *corrected* through stellar optopolarimetry. Polarization of starlight in-

duced by dichroic dust absorption traces the direction of the magnetic field in intervening absorbing clouds (Hildebrand 1999). If the optopolarimetric properties of many (tens) of stars within a single CMB B-mode beam were measured, and if these stars were located at various, known distances, then the magnetic field direction in the various clouds along each line of sight could be determined. Such *magnetic tomography* of the interstellar medium could immediately identify lines of sight with severe misalignments of the magnetic field along the line of sight, and these lines of sight could be simply masked from B-mode analyses, akin to the treatment of point sources. In the era of Gaia (e.g., Bailer-Jones et al. 2013) which will provide distance measurements to stars down to 20th magnitude, the bottleneck in such an endeavor will be the number of high-accuracy optopolarimetric measurements that can be performed down to very low polarization fractions characteristic of the regions targeted by CMB experiments.

ACKNOWLEDGMENTS

We thank A. Readhead, B. Hensley, N. Kylafis, P. Goldsmith, G. Panopoulou, A. Tritsis, and I. Lioudakis for useful comments. We thank an anonymous referee for a constructive review. We acknowledge support by: the “RoboPol” project, implemented under the “ARISTEIA” Action of the “OPERATIONAL PROGRAMME EDUCATION AND LIFELONG LEARNING”, co-funded by the European Social Fund (ESF) and Greek National Resources; the European Commission Seventh Framework Programme (FP7) through grants: PCIG10-GA-2011-304001 “JetPop”; PCIG-GA-2011-293531 “SFOnset”; PIRSES-GA-2012-31578 “EuroCal”.

REFERENCES

- André, P., Men’shchikov, A., Bontemps, S., et al. 2010, *A&A*, 518, LL102
 Bailer-Jones et al. 2013, *A&A*, 559, A74
 Bicep2 Collaboration. 2014, *Physical Review Letters*, 112, 241101
 Hildebrand, R. H. 1983, *QJRAS*, 24, 267
 Hildebrand, R. H. 1999, in *ApSS Library*, Vol. 241, *mm-wave Astronomy: Molecular Chemistry & Physics in Space*, ed. W.Wall, A. Carramiñana, & L. Carrasco, 115
 Lenz, D., Kerp, J., Flöer, L., et al. 2015, *A&A*, 573, AA83
 Peek, J. E. G., Heiles, C., Peek, K. M. G., Meyer, D. M., & Lauroesch, J. T. 2011, *ApJ*, 735, 129
 Planck Collaboration, Abergel, A., Ade, P. A. R., et al. 2014, *A&A*, 571, AA11
 Planck Collaboration. 2014a, *A&A*, 566, A55
 Planck Collaboration, Ade, P. A. R., Aghanim, N., et al. 2014, arXiv:1405.0872
 —. 2014b, ArXiv e-prints 1405.0874
 —. 2014c, arXiv:1409.2495
 —. 2014d, ArXiv e-prints 1409.5738
 BICEP2/Keck, Planck Collaborations, :, et al. 2015, arXiv:1502.00612
 Serkowski, K., Mathewson, D. S., & Ford, V. L. 1975, *ApJ*, 196, 261